Chapter 11 Coherence Editing: Pulse-field Gradients and Phase Cycling

Coherence editing is used to remove unwanted signals from NMR spectra. For example, in the double quantum filtered COSY experiment, to suppress signals from uncoupled protons, such as the intense solvent line, while retaining signals from coupled spins. This filtering is accomplished by distinguishing between the different quantum states of the magnetization during the experiment: uncoupled spins can only attain a single-quantum state while coupled spins can be in a double-quantum state during the experiment.

Coherence editing is accomplished by encoding different states with a unique phase during the pulse sequence. The selection of a desired state is attained by detecting only those signals with the appropriate phase. The phase encoding of the signal can be accomplished by either phase cycling of RF-pulses or by the application of short pulses of spatially varying magnetic fields, otherwise known as pulsed-field gradients (PFG), during evolution delays.

In the case of phase cycling, multiple scans are acquired with the phase of pulses and the receiver altered in a systematic fashion such that the desired signals (e.g. double-quantum) are always co-added while the undesired signals (e.g. single quantum states) add to zero at the end of the phase cycle, as illustrated in Panel A of Fig. 11.1.

In the case of using pulsed-field gradients for coherence editing, a spatially varying magnetic field is used to impart a characteristic phase shift on both the desired and undesired signals. The amount of phase shift depends on the quantum level of the spins. For example, the phase shift encoded in a single-quantum term would be half of that encoded in a double-quantum term. The retention of the desired signal and discarding of the undesired signal is simply accomplished by refocusing (returning the phase shift to zero) the desired signal.

Both phase cycling and magnetic field gradients can effectively suppress undesirable signals. Magnetic field gradients tend to be more effective than phase cycling methods because they can be applied in a single scan, thus scan-to-scan reproducibility of the instrument is not a critical factor.

In addition, suppression of strong solvent signals can also be accomplished within a single scan, greatly reducing the dynamic range of the acquired signals, resulting in more accurate conversion of the analog signal to digital form. In addition, the requirement of acquiring multiple scans with phase cycling can lead to an undesirable increase in the length of the experiment, especially in the case of three- or four-dimensional experiments.

There are two significant disadvantages associated with pulsed-field gradients. First, additional delays have to be incorporated into the pulse sequence for the application of gradients. In some cases this is not possible due to timing constraints. Second, there can be an inherent reduction in sensitivity because the portion of the magnetization that is rejected by the field gradients may contain useful signal. Consequently, most experiments utilize a combination of pulsed-field gradients and phase cycling to remove undesirable signals from the spectrum.

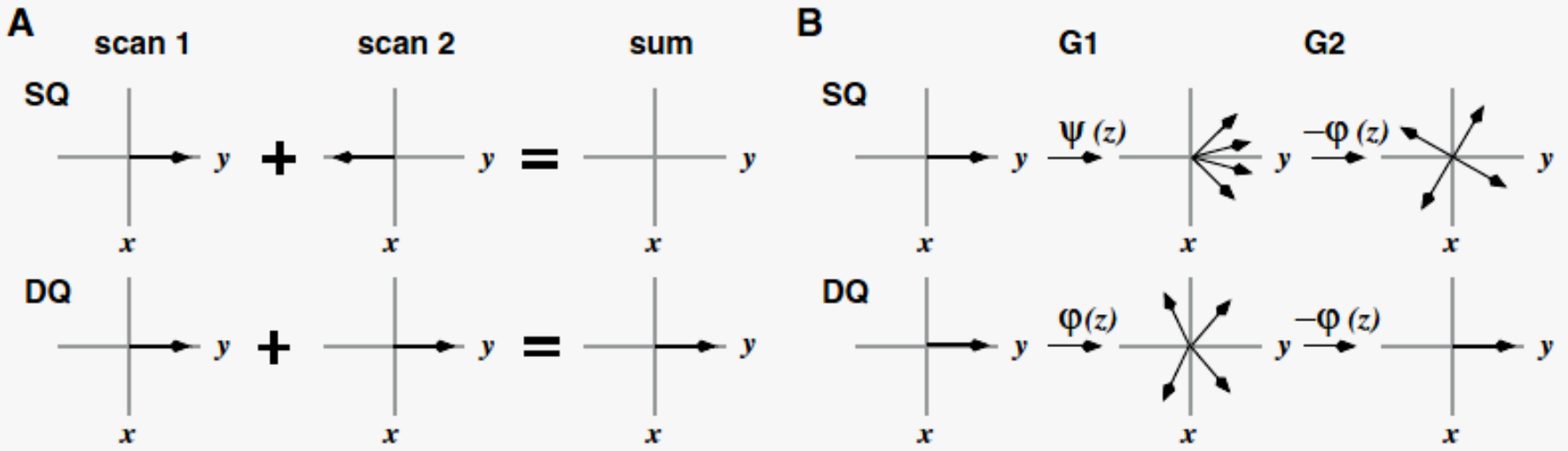

Figure 11.1. Coherence editing in the DQF-COSY experiment. Panel A illustrates coherence editing by phase cycling while Panel B shows editing using pulsed magnetic field gradients. In both cases, the signal associated with the double quantum (DQ) state is retained while that from the single quantum state (SQ) is rejected. In the case of phase cycling (A), two scans are acquired and summed. The phase of the signal associated with the DQ state differs from that of the SQ such that when the signals are added, the DQ signals add while the SQ signals cancel. In the case of coherence editing using pulsed-field gradients, the magnetization associated with the DQ state receives a phase shift of $\varphi(z)$ due to the application of the first field gradient (G1). The actual phase shift depends on the z-coordinate of the nuclear spin in the sample. In contrast, the SQ state acquires a different phase shift ($\psi(z)$). A second gradient (G2) is designed to reverse the phase shift associated with the DQ state, rendering it detectable. In contrast, the magnetization associated with the SQ state is not refocused, such that the signal averaged over the ensemble of spins is zero. Note that the coherence editing is accomplished within a single scan.

11.1 Principals of Coherence Selection: 11.1.1 Spherical Basis Set

The product operator representation of the density matrix using Cartesian angular momentum operators, such as I_x, has proven to be very convenient for the analysis of the effect of RF-pulses on the density matrix during an NMR experiment. However, the Cartesian representation is cumbersome for analyzing the effect of phase cycling or field gradients on the density matrix. Instead, we will adopt a different representation of the density matrix in which the basis set will represent individual transitions, or coherences, of the system. This basis set is often referred to as a spherical basis set.

Table 11.1. Spherical and Cartesian Basis Set. The relationship between the spherical and Cartesian basis set is presented. The property of the system that is associated with each of the spherical basis elements is also given.

Spherical	*Cartesian Representation*	*Description*
σ^0	I_z	Population difference P_e-P_g
σ^{+1}	$I_x + iI_y$	Upward transition $\Phi_g \rightarrow \Phi_e$
σ^{-1}	$I_x - iI_y$	Downward transition $\Phi_e \rightarrow \Phi_g$

For a single uncoupled spin the correspondence between the Cartesian and the spherical basis set is shown in Table 11.1. The density matrix, σ^o represents the equilibrium population difference between the ground and excited states and is referred to as zero-quantum coherence. Single quantum coherences are represented by σ^{+1}, which represents systems in transition from the ground to the excited state, and σ^{-1}, which represents transitions from the excited to the ground state.

The fact that the spherical basis set represents transitions in a single direction can be clearly seen from their corresponding density matrices:

$$\sigma^{+1} = \frac{\hbar}{2}\begin{bmatrix} 0 & 1 \\ 0 & 0 \end{bmatrix} \qquad \sigma^{-1} = \frac{\hbar}{2}\begin{bmatrix} 0 & 0 \\ 1 & 0 \end{bmatrix} \tag{11.1}$$

while the Cartesian representation generally represent both upward and downward transitions, for example:

$$I_x = \frac{\hbar}{2}\begin{bmatrix} 0 & 1 \\ 1 & 0 \end{bmatrix} \tag{11.2}$$

The Cartesian representation of the density matrix can be converted to the spherical representation using the following transformations:

$$I_x = \frac{1}{2}[\sigma^{+1} + \sigma^{-1}] \qquad I_y = \frac{1}{2i}[\sigma^{+1} - \sigma^{-1}] \tag{11.3}$$

11.1.1.1 Selection of Double Quantum Coherence in DQF-COSY Experiment

As an example of the selection of particular transition by phase cycling or pulsed-field gradients, consider the magnetization present in the DQF-COSY experiment during the delay Δ (See Fig. 9.10).

$$\begin{aligned} 2I_xS_y &= 2\frac{1}{2}(I^+ + I^-)\frac{1}{2i}(S^+ - S^-) \\ &= \frac{1}{2i}[I^+S^+ - I^+S^- + I^-S^+ - I^-S^-] \end{aligned} \tag{11.4}$$

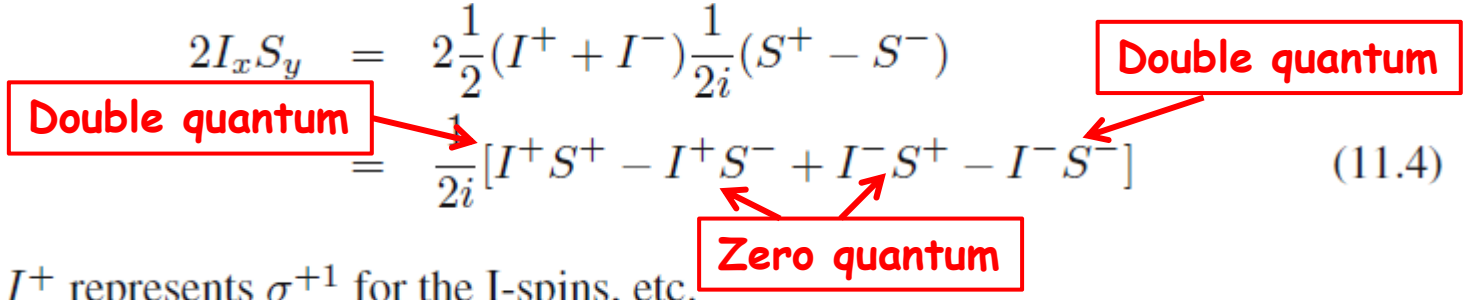

where I^+ represents σ^{+1} for the I-spins, etc.

The density matrices I^+S^+ and I^-S^- are non-zero for only elements that represent double quantum transitions while the matrices I^+S^- and I^-S^+ have only non-zero elements that represent zero quantum transitions. Consequently, this Cartesian form of the density matrix $(2I_xS_y)$ can be expressed using the spherical basis set as:

$$\rho = \sigma^{+2} + \sigma^0 + \sigma^{-2}$$

Coherence selection, either by pulsed-field gradients or phase cycling of pulses, would induce a phase shift in each of the separate coherences at this point in the experiment. The phase encoding depends on the coherence level of each element of the density matrix. After application of gradients, or phase alteration of the pulses, the above density matrix would have the form:

$$\rho = \sigma^{+2}e^{i\varphi_2} + \sigma^0 e^0 + \sigma^{-2}e^{-i\varphi_2}$$

where φ_2 is the phase shift associated with the σ^{+2} part of the density matrix. Note that the shift associated with the σ^{-2} term is exactly opposite to the phase shift of σ^{+2}.

If a second phase shift of $e^{-i\varphi_2}$ is induced in the signal, by the application of a gradient at some time later in the sequence, or by altering the receiver phase in the case of phase cycling, then the density matrix will become:

$$\rho = e^{-i\varphi_2}[\sigma^{+2}e^{i\varphi_2} + \sigma^0 e^0 + \sigma^{-2}e^{-i\varphi_2}] = \sigma^{+2} + \sigma^0 e^{-2i\phi} + \sigma^{-2}e^{-i2\varphi_2}$$

If we then assume that only signals with a phase shift of zero can be detected, then the final density matrix consists only of signals that were in a double-quantum state during the Δ period, all other signals will be absent from the spectrum.

The above example represents the general nature of coherence selection by phase cycling or pulsed-field gradients. In both cases the elements of the density matrix are encoded with a known phase shift, and this phase shift is exploited to reject all of the undesirable signals.

11.1.2 Coherence Changes in NMR Experiments

Before coherence selection methods can be applied to an NMR experiment it is necessary to know the coherences that are present during the experiment. Any NMR experiment can be considered to be a series of pulses that bracket periods of free evolution. Since periods of free evolution correspond to a rotation about the z-axis, there is no change in the coherence level during those periods, the density matrix simply develops a phase shift that is proportional to the frequency of the transition that is represented by each element of the density matrix, e.g. $\sigma^{+1} \rightarrow \sigma^{+1}e^{-i\omega t}$. In contrast, RF-pulses create new coherence levels in a system by virtue of the fact that they cause transitions between spin states.

11.1.2.1 Example - Coherence Order in a COSY Experiment

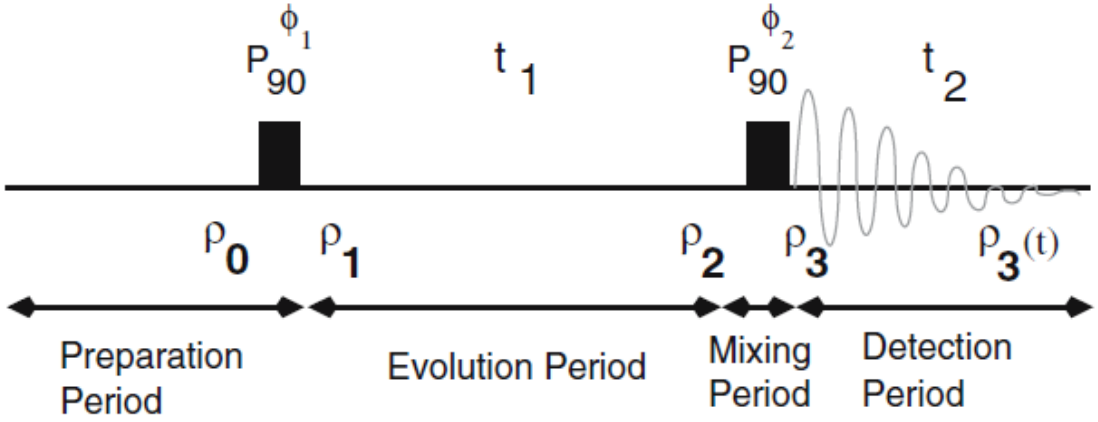

The initial state of the system is:

$$\rho_0 = \sigma^0 = I_z + S_z = \begin{bmatrix} 1 & 0 & 0 & 0 \\ 0 & 0 & 0 & 0 \\ 0 & 0 & 0 & 0 \\ 0 & 0 & 0 & -1 \end{bmatrix}$$

After the first pulse:

$$\rho_1 = -I_y - S_y = \begin{bmatrix} 0 & -i & -i & 0 \\ i & 0 & 0 & -i \\ i & 0 & 0 & -i \\ 0 & i & i & 0 \end{bmatrix} \propto I^+ + I^- + S^+ + S^- = \sigma_I^1 + \sigma_I^{-1} + \sigma_S^1 + \sigma_S^{-1}$$

This density matrix is composed of an equal mixture of σ^{+1} and σ^{-1} coherences for both the I and S spins. During the t_1 evolution time the density matrix evolves under both J-coupling and chemical shift evolution. At the end of t_1 the part of the density matrix that will give rise to the crosspeak is:

$$\rho_2 = 2I_y S_z sin(\omega_I t_1) sin(\pi J t_1)$$

This is still a mixture of single quantum coherences, as indicated by the presence of only one transverse operator (I_y). Therefore, evolution of the system under either the chemical shift or the J-coupling Hamiltonian does not change coherence order, as discussed above.

The final pulse of the COSY experiment exchanges magnetization between the two coupled spins:

$$2I_y S_z \rightarrow -2I_z S_y$$

The detected signal is obtained in the usual fashion, by taking the trace of the density matrix and the operator that represents the observable. In the case of quadrature detection the observable for the I spin is $I^+ = I_x + iI_y$ (a similar expression could be written for the S spins), giving the following signal:

$$M^+(t) = M_x(t) + iM_y(t) = \text{Trace}\left[\,\rho(I_x + iI_y)\right] = \text{Trace}\left[\,\rho I^+\right]$$

Recall that; $$I^+ = \begin{bmatrix} 0 & 0 & 1 & 0 \\ 0 & 0 & 0 & 1 \\ 0 & 0 & 0 & 0 \\ 0 & 0 & 0 & 0 \end{bmatrix} \quad \text{and} \quad I^- = \begin{bmatrix} 0 & 0 & 0 & 0 \\ 0 & 0 & 0 & 0 \\ 1 & 0 & 0 & 0 \\ 0 & 1 & 0 & 0 \end{bmatrix}$$

Therefore, the only density matrix that gives a non-zero trace when multiplied by I^+ is I^-. Consequently, the only coherence state that is detected with quadrature detection is σ^{-1}.

In summary, in the COSY experiment, the density matrix can be represented by zero quantum coherence prior to the first pulse, as single quantum coherence during t_1, and the detected signal is proportional to the contribution of -1 coherence to the density matrix.

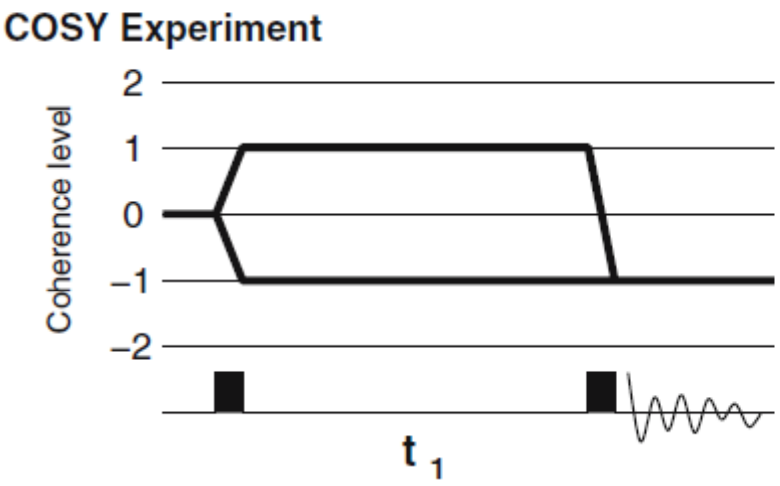

Figure 11.2 Coherence changes in the COSY experiment. The desired coherence changes in the COSY experiment are summarized with a coherence level diagram. The initial coherence level is zero (σ^0), the first pulse generates both σ^{+1} and σ^{-1} for both I and S spins. The second mixing pulse interchanges the label associated with each coherence (e.g. $\sigma_I^{+1} \rightarrow \sigma_S^{+1}$) and at the end of the experiment, only σ^{-1} is detected by quadrature detection.

11.1.3 Coherence Pathways

The coherence changes that occurred during the COSY experiment are neatly summarized by a coherence pathway diagram, as shown in Fig. 11.2. The system begins in a zero-quantum state, representing populations, is then transformed to single quantum states by the first pulse, followed by detection of -1 single quantum coherence after the second pulse. These transformations of the density matrix can also be represented by the following sets of *coherence paths*:

$$\sigma^0 \rightarrow \sigma^{+1}(t_1) \rightarrow \sigma^{-1} \qquad\qquad \sigma^0 \rightarrow \sigma^{-1}(t_1) \rightarrow \sigma^{-1}$$

The above coherence changes specify the *desired* changes in coherence during the COSY experiment. There are other coherence paths that are also present. These paths are undesired because they can lead to the presence of unwanted artifacts in the final spectra. For example, if the first RF-pulse was not exactly equal to 90°, then the first pulse will leave some magnetization along the z-axis, which is represented by zero quantum coherence. Therefore, the following pathway is one of a number of *undesirable* coherence pathways that can occur in the COSY experiment:

$$\sigma^0 \rightarrow \sigma^0 \xrightarrow{t_1} \sigma^0 \rightarrow \sigma^{-1}$$

Having defined the desired coherence changes in the COSY experiment, the following sections will illustrate how pulsed-field gradients (Section 11.2) or RF-pulse phase shifts (Section 11.3) can be used to select the desired coherence changes in an experiment while rejecting the undesired ones.

11.2 Phase Encoding With Pulsed-Field Gradients

11.2.1 Gradient Coils

To employ pulsed-field gradients in coherence editing it is necessary to use specially designed probes and electronics. In the case of the probe, one (z-gradient) or three (triple-axis: x, y, z-gradients) additional coils are placed next to the sample. Each coil will generate a magnetic field gradient within the sample when current is passed through the coil. The gradient coils are designed in such a manner that the generated B_z field depends on the *position* of the nuclear spin within the sample tube. For example, a triple axis gradient would generate the following magnetic field at a position (x, y, z) in the sample:

$$B_z = G_z \times z + G_x \times x + G_y \times y$$

where G_i represents the gradient strength in the i direction, or the change in the magnetic field in the z-direction due to a change in the coordinate in the i^{th} dimension:

$$G_i = \partial G_i / \partial x_i$$

The applied gradients can be either positive or negative, are of a well defined amplitude, and can be activated for well defined periods of time using simple commands within the NMR pulse program.

11.2.1.2 Effect of Position on Gradient Induced Phase Changes

During the application of a magnetic field gradient along the z-axis, the magnetic field will become $B_z = B_o + G_z \cdot z$. Therefore the precessional frequency of a spin will become:

$$\omega = \omega_s + \gamma G_z \times z$$

If the field gradient is applied for a period τ, then the evolution of the density matrix by the end of the gradient pulse is given by:

$$\rho(\tau) = e^{-i\omega\tau I_z} \rho e^{+i\omega\tau I_z}$$

corresponding to a rotation about the z-axis by an angle $\omega\tau$.

Different molecules in the NMR tube will experience different field strengths during the application of a magnetic field gradient because of their different locations within the sample. The effect of a simple z-gradient on the phase of spins is shown in Fig. 11.3. In this figure the nuclear spins labeled 'E' are at the center of the sample and do not precess in the rotating frame. Spins that are spatially above E experience a stronger magnetic field and therefore precesses more rapidly than the rotating frame, moving in a counter-clockwise direction. As spins become more distant from E (e.g. position H) the precessional rate increases because of the field gradient. In a similar manner, spins that are below 'E' in the sample experience a weaker magnetic field and

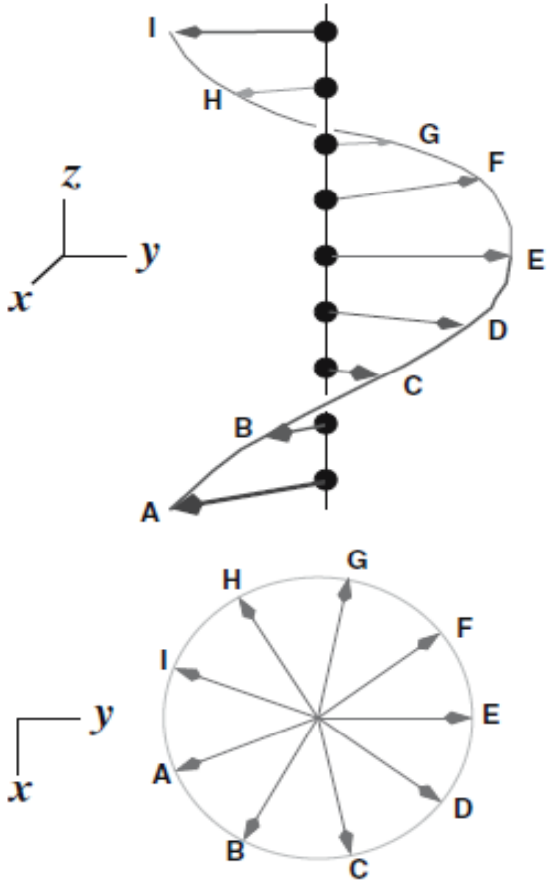

Figure 11.3 Effect of magnetic field gradients on the precessional rate of spins. This figure illustrates the effect of a field gradient along the z-axis. The top section of the figure is a side view of the sample and the bottom section provides a top view of the sample. The magnetization was initially along the y-axis in the rotating frame. The rate of rotation is such that spins at position 'E' are on resonance and therefore do not evolve. The middle of the sample, at $z = 0$ (E), experiences no change in field while the gradient is applied. The magnetic field increases as the displacement from the center increases. Spins above 'E' experience a larger field and spins below 'E' experience a smaller field. The direction of the arrows mark the position of the transverse magnetization after the application of the gradient.

11.2.2 Effect of Coherence Levels on Gradient Induced Phase Changes

$$e^{-i\phi I_z}\sigma^{+1}e^{i\phi I_z} = e^{-i\phi I_z}(I_x + iI_y)e^{i\phi I_z} = I_x cos\phi + I_y sin\phi + i\,[I_y cos\phi - I_x sin\phi]$$
$$= I_x(cos\phi - isin\phi) + I_y(sin\phi + icos\phi) = I_x e^{-i\phi} + iI_y(cos\phi - isin\phi)$$
$$= (I_x + iI_y)e^{-i\phi} = \sigma^{+1}e^{-i\phi}$$

In a similar manner:

$$e^{-i\phi I_z}\sigma^{-1}e^{i\phi I_z} = \sigma^{-1}e^{+i\phi}$$
$$e^{-i\phi(I_z+S_z)}\sigma^{0}e^{i\phi(I_z+S_z)} = \sigma^{0}$$
$$e^{-i\phi(I_z+S_z)}\sigma^{+2}e^{i\phi(I_z+S_z)} = \sigma^{+2}e^{-2i\phi}$$

Generalizing from the above calculations, if a z-rotation of magnitude ϕ is applied to a coherence of level p, then the coherence will be phase shifted by $e^{-ip\phi}$, that is:

$$\sigma^p \xrightarrow{\phi} \sigma^p e^{-i\ p\phi}$$

11.2.2.1 Example: Coherence Selection in a DQF-COSY Using Gradients

The coherence level diagram for the DQF-COSY experiment is shown in Fig. 11.4. One of the desired coherence paths is:

$$\sigma^0 \rightarrow \sigma^{+1} \rightarrow \sigma^{+2} \rightarrow \sigma^{-1}$$

This pathway can be selected by utilizing a total of three gradient pulses, one during t_1, one during the Δ period and one during detection to refocus the desired coherence path, as illustrated in Fig. 11.4. The first gradient will label the single quantum coherence with a phase shift of: $\phi = -(+1)\gamma G_z \tau$

The second gradient, of the same strength and length as the first, will induce an additional phase shift of $\phi = -2 \times \gamma(-G_z)\tau$ in the part of the density matrix that is represented by σ^{+2}. Therefore, the overall induced phase shift after the second gradient pulse is:

$$\phi = -[1+2]\gamma G_z \tau$$

After the application of the third RF-pulse it will be necessary to refocus this phase shift by applying a third gradient. At this point in the experiment the desired density matrix has a phase shift of $\phi = -[1+2]\gamma G_z \tau$ associated with it. Therefore a phase shift of opposite sign has to be induced in the density matrix. This can be attained by the application of a gradient that is either three times the length of the first gradient, or one that is three times as strong. This gradient induces the following change in σ^{-1}:

$$\sigma^{-1} e^{-[1+2]\gamma G_z \tau} \xrightarrow{G_3} \sigma^{-1} e^{+3\gamma G_z \tau} e^{-[1+2]\gamma G_z \tau} = \sigma^{-1}$$

Therefore, only magnetization that follows the coherence levels of +1, +2, and -1 will be refocused by the last gradient pulse and give rise to a detectable signal.

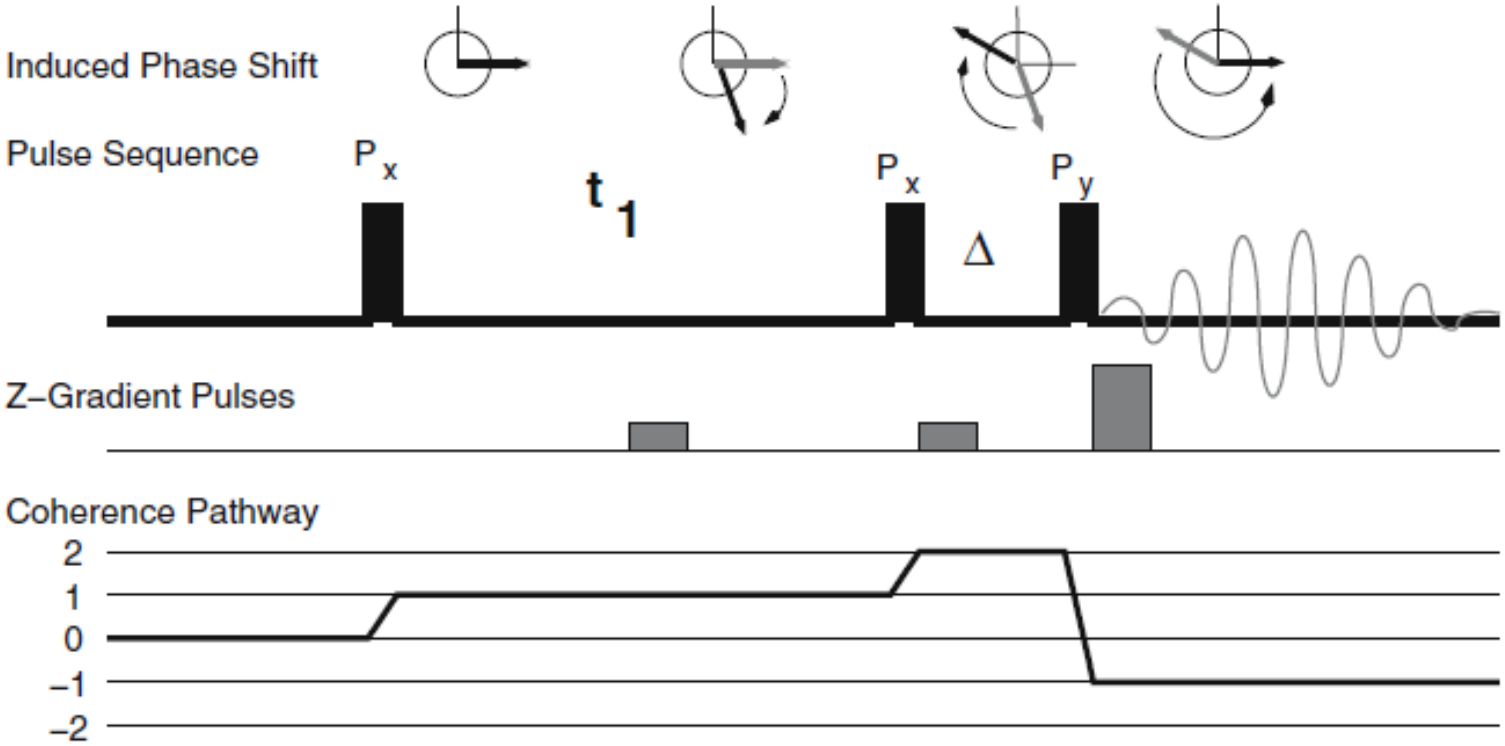

Figure 11.4. Coherence selection in a DQF-COSY experiment using gradients. One of the desired coherence pathways in a DQF-COSY experiment is highlighted by a thick line on the coherence scale shown in the lower part of the figure. Three field gradients are applied for coherence selection, one during t_1, one during the delay Δ, and one at the beginning of the acquisition time. The gradients are all positive in this example. The induced phase shifts for a particular position within the sample are shown on the top of the diagram. The first gradient induces a 70° phase shift. The second gradient increases the phase shift to 210° $(70 + 140)$. The last gradient pulse reverses the phase shift that was induced by the first two gradients, resulting in detectable signal from this particular coherence path.

11.2.3 Coherence Selection by Gradients in Heteronuclear NMR Experiments

Pulsed-field gradients can also be used to select particular coherence paths in heteronuclear NMR experiments. For example, consider the HSQC pulse sequence shown in Fig. 11.5. The application of two gradient pulses, G_1 and G_2 will select coherence paths in which the magnetization is transverse on the X-spin during t_1 and then transverse on the proton during detection. Both gradient pulses are applied within a spin-echo sequence (e.g. $\tau - 180° - \tau$) to prevent chemical shift evolution during the application of the gradient. In the case of the first gradient pulse, the spin-echo delay need only be as long as G_1 plus its recovery time. In the case of the second gradient pulse, the gradient is applied during the normal proton-heteronuclear refocusing period, τ.

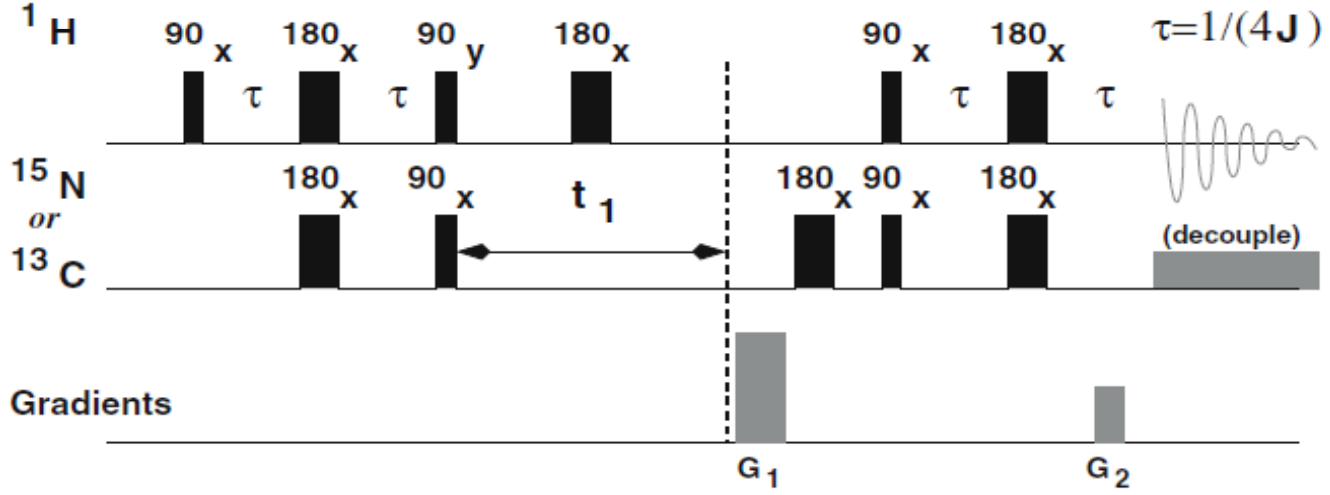

Figure 11.5. Use of pulsed-field gradients for coherence path selection in a HSQC experiment. The application of the first gradient (G_1) induces a phase shift in the various coherences that comprise the density matrix. If the ratio of the two gradients is γ_X / γ_H, then heteronuclear single quantum coherence that is present during t_1 is refocused as detectable proton magnetization by the second gradient.

During the t_1 evolution time the density matrix that represents the heteronuclear magnetization consists of σ^{+1} and σ^{-1}. Application of the first gradient, G_1, will induce a phase shift of $e^{-1\gamma_X G_1}$ and $e^{+1\gamma_X G_1}$, respectively, in each of these coherences. The factor γ_X is explicitly written to take into account the fact that the precessional frequency is proportional to γ (See Eq. 11.18). The second gradient will induce a phase shift of $e^{+1\gamma_H G_2}$ in the detectable proton magnetization, σ_H^{-1}. If the gradient strengths are adjusted such that

$$\frac{G_1}{G_2} = \frac{\gamma_H}{\gamma_X} \tag{11.30}$$

then the phase shift induced in σ_X^{+1} at the end of t_1 will be refocused by the gradient applied during the second INEPT period. Consequently, the only magnetization that will give rise to a detectable signal must have been transverse and associated with the X-spin during t_1 and then transfered to the proton for detection.

11.2.3.1 Coherence Rejection by Pulse-Field Gradients (z-filters)

Direct selection of individual coherences is very effective at suppressing unwanted signals. Unfortunately, direct selection of coherence leads to loss of signal because the phase shift that is induced in the σ^{-1} component of the density matrix by the first gradient pulse *cannot* be rephased by the second gradient. Consequently, one-half of the signal is lost by the gradient selection. Signal loss can be avoided by utilizing gradients to dephase unwanted coherences without affecting the desired coherences [15]. Recall that zero-quantum coherences (σ^o) are not affected by field gradients. Consequently, if the desired magnetization is stored along the z-axis during the application of a gradient pulse, it will not be affected by the gradient. In the case of a single spin, a gradient will have no effect when $\rho = I_z$. For two spins, a gradient will have no effect when $\rho = 2I_zS_z$. Gradient pulses that are applied to retain z-states of the

magnetization are referred to as z-filters in the case $\rho = I_z$, and zz-filters in the case of $\rho = 2I_zS_z$.

The application of this technique to the HSQC experiment is illustrated in Fig. 11.6. Note that the 90° proton and heteronuclear pulses are no longer applied simultaneously, but are now offset from each other and a field gradient pulse has been applied between the two RF-pulses. During this period, the desired component of the density matrix is along the z-axis. For example, at the end of the first INEPT period the density matrix is: $\rho = 2I_xS_z$

the 90° proton pulse along the y-axis converts this to: $\rho = 2I_zS_z$

which is not affected by the applied pulsed-field gradient. The solvent signal, on the other hand, will be transverse during the application of the gradient and will thus receive a spatially dependent phase shift that will greatly attenuate its contribution to the final detected signal.

11.2.3.2 Reduction of Artifacts in 180° Pulses with Field Gradients.

Refocusing pulses in heteronuclear experiments can introduce artifacts into the spectrum if they do not completely invert the spins. Placement of a matched pair of gradient pulses on either of side of the 180° pulse will dephase artifacts that are generated from a non-ideal pulse. Examples of this technique are shown in Fig. 11.6, involving pairs of gradients G1 and G2 plus G5 and G6.

It is easy to show that the pair of gradients has no effect on the desired evolution of magnetization during these periods. Prior to the pulse, the density matrix associated with the proton magnetization is:

$$\rho = \sigma^{+1} + \sigma^{-1}$$

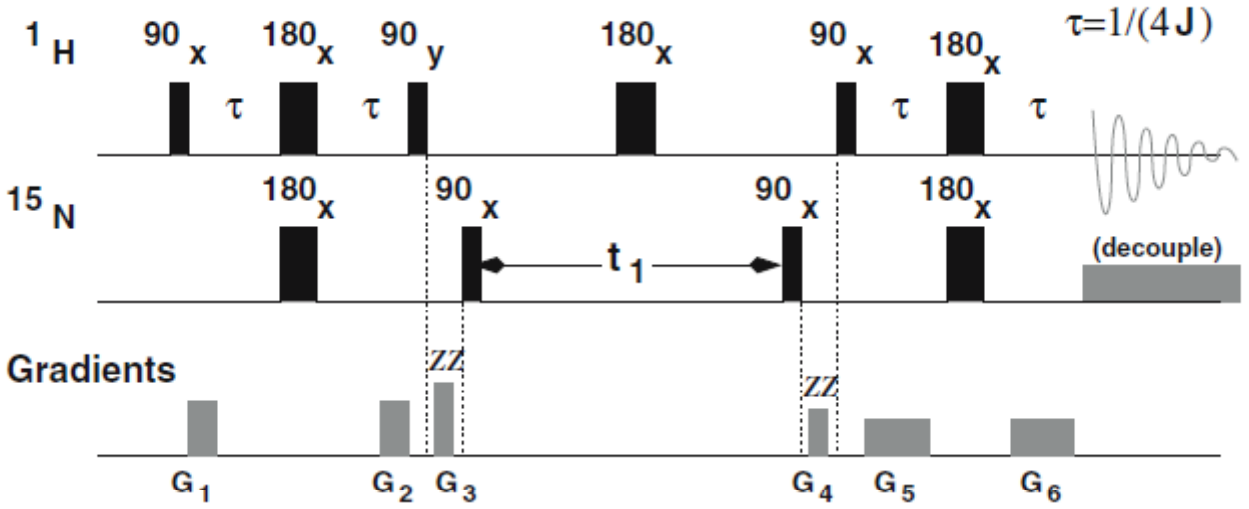

Figure 11.6. Artifact suppression with pulsed-field gradients in heteronuclear experiments.

Pulsed-field gradients can be used to suppress artifacts by either the rejection of coherences (z-filter) or by the symmetrical placement of gradient pulses around 180° pulses. The two gradient pulses that act as zz-filters are G_3 and G_4. These are usually of different strengths such that G_4 does not accidentally refocus magnetization that was defocused by G_3. G_1 and G_2 serve to remove artifacts from the 180° proton and heteronuclear pulses during the first INEPT period. These two gradients *must* be the same amplitude. Gradient pulses G_5 and G_6 serve the same purpose during the second INEPT period. This pair of gradient pulses must also have the same amplitude, however the amplitudes of the G_1, G_2 pair need not be the same as the G_5, G_6 pair. Note that all of these gradient pulses have no effect on the normal magnetization transfers associated with the HSQC experiment, they simply remove artifacts and signals from protons that are not coupled to heteronuclear spins.

After the first gradient, but before the 180° pulse, a phase shift, G, has been induced in the magnetization by the gradient, giving:

$$\rho = \sigma^{+1} e^{-iG} + \sigma^{-1} e^{+iG}$$

The 180° pulse interchanges the values +1 and -1 coherences, as follows:

$$\begin{bmatrix} 0 & e^{-iG} \\ e^{+iG} & 0 \end{bmatrix} \xrightarrow{P_{180}} \begin{bmatrix} 0 & e^{+iG} \\ e^{-iG} & 0 \end{bmatrix}$$

giving the density matrix after the 180° pulse, but before the second gradient,

$$\rho = \sigma^{+1} e^{+iG} + \sigma^{-1} e^{-iG}$$

After the second gradient, these phase shifts are reversed, giving the original density matrix:

$$\rho = \sigma^{+1} e^{-iG} e^{+iG} + \sigma^{-1} e^{+iG} e^{-iG} = \sigma^{+1} + \sigma^{-1} \qquad (11.37)$$

However, in the case of an imperfect pulse, some of the transverse magnetization may be converted to longitudinal magnetization. Since longitudinal magnetization is not affected by the second field gradient (σ^0) its phase will not be refocused by the second gradient and will not appear as observable magnetization.

11.3 Coherence Selection Using Phase Cycling

Phase cycling involves acquiring and co-adding the free induction decays from a number of experiments that are identical in all aspects, except the phases of one or more RF-pulses and the phase of the receiver. In contrast to field gradients, coherence editing is not obtained within a single scan, rather it is the summation of the data from all of the individual scans that results in the cancellation of unwanted signals. For example, if an experiment uses a four step phase cycle for one of the pulses then four individual FIDs will be acquired with pulse phases of 0, π/2, π, and 3π/2. *These four* FIDs are added together such *that* the signal associated with the desired coherence path add constructively while signals associated with undesired paths are canceled by the summation

11.3.1 Coherence Changes Induced by RF-Pulses

The application of RF-pulses to the spins generates new coherence levels from existing ones. For example, if the first 90° pulse in the COSY or DQF-COSY experiment is ideal, it will cause the following changes in coherences:

$$\sigma^0 \xrightarrow{P_1} \sigma^{+1} + \sigma^{-1}$$

In general, the effect of a pulse, P_i, on a single coherence is to generate a manifold of coherences:

$$P_i \sigma^p(t_i^-) P_i^{-1} = \sum_{p'} \sigma^{p'}(t_i^+) \tag{11.39}$$

where $\sigma^p(t_i^-)$ represents the density matrix before the pulse, and $\sum_{p'} \sigma^{p'}(t_i^+)$ represents ρ after the pulse.

The key to coherence editing using phase cycling is that a change in phase of the pulse will produce a phase shift of the coherences that are produced by the pulse, providing a means to label each coherence with a known phase shift.

11.3.1.1 Phase Shifts of Pulses are Z-rotations

To determine how changing the phase of the pulse generates a phase shift of coherence levels it is necessary to write a general expression for a phase shifted pulse and then evaluate the effect of this pulse on an arbitrary coherence level.

A change in the phase of a pulse is equivalent to the rotation about the z-axis of the operators that describe the pulse. For example, if the phase of a excitation pulse in an experiment is cycled in the following manner, $\mathrm{P}_x, \mathrm{P}_y, \mathrm{P}_{-x}, \mathrm{P}_{-y}$

Then the pulse along the y-axis is related to the original pulse along the x-axis by a $90°(\pi/2)$ rotation about the z-axis, as follows:

$$P_y = e^{-iI_z \frac{\pi}{2}} P_x e^{iI_z \frac{\pi}{2}}$$

In a similar manner, the pulse along the minus x-axis is obtained by applying a $180°(\pi)$ rotation to the original pulse: $P_{-x} = e^{-iI_z\pi} P_x e^{iI_z\pi}$

The effect of phase shifted pulses on the density matrix is obtained by applying the rotated pulse to the density matrix. For example, if an arbitrary density matrix, ρ, is transformed to ρ_x by an x-pulse with a flip angle of β as follows:

$$e^{-i\beta I_x} \rho e^{i\beta I_x} \rightarrow \rho_x$$

then the effect of a y-pulse on the same initial density matrix is given by:

$$\left[e^{-iI_z\pi/2} e^{-i\beta I_x} e^{iI_z\pi/2}\right] \rho \left[e^{-iI_z\pi/2} e^{i\beta I_x} e^{iI_z\pi/2}\right] \rightarrow \rho_y \qquad (11.43)$$

This equation can be written for any arbitrary pulse, P_o, phase shifted by any arbitrary amount, ϕ:

$$e^{-i\phi I_z} P_o e^{+i\phi I_z} \rho e^{-i\phi I_z} P_o^{-1} e^{+i\phi I_z} \rightarrow \rho_\phi \qquad (11.44)$$

Since any density matrix, ρ, can always be written as a linear sum of difference coherences (e.g. $\rho = \sum_{p=-n}^{+n} a_p \sigma^p$) it is possible to simplify the analysis by considering a single arbitrary coherence, σ^p.

Recalling that the effect of z-rotations on coherence levels is:

$$e^{-i\phi I_z} \sigma^p e^{+i\phi I_z} = \sigma^p e^{-ip\phi}$$

then, the following is true: $e^{+i\phi I_z} \sigma^p e^{-i\phi I_z} = \sigma^p e^{+ip\phi}$

The following shows the effect of a phase shifted pulse when applied to a coherence level of p, to give ρ_ϕ:

$$\begin{aligned}\rho_\phi &= \left[e^{-i\phi I_z} P_o e^{+i\phi I_z}\right] \sigma^p \left[e^{-i\phi I_z} P_o^{-1} e^{+i\phi I_z}\right] \\ &= e^{-i\phi I_z} P_o \left[e^{+i\phi I_z} \sigma^p e^{-i\phi I_z}\right] P_o^{-1} e^{+i\phi I_z} \\ &= e^{-i\phi I_z} P_o \left[\sigma^p e^{+ip\phi}\right] P_o^{-1} e^{+i\phi I_z} \\ &= e^{-i\phi I_z} \left[P_o \sigma^p P_o^{-1}\right] e^{+i\phi I_z} e^{+ip\phi}\end{aligned} \tag{11.47}$$

Assuming that the application of a pulse to a single coherence generates a manifold of different coherences after the pulse: $P_o \sigma^p P_o^{-1} \rightarrow \sum_{p'} \sigma^{p'}$

then,

$$\begin{aligned}\rho_\phi &= e^{-i\phi I_z} \sum_{p'} \sigma^{p'} e^{i\phi I_z} e^{+ip\phi} \quad = \sum_{p'} \left[e^{-i\phi I_z} \sigma^{p'} e^{+i\phi I_z}\right] e^{+ip\phi} \\ &= \sum_{p'} \sigma^{p'} e^{-ip'\phi} e^{+ip\phi} \quad = \sum_{p'} \sigma^{p'} e^{-i\Delta p\phi}\end{aligned} \tag{11.48}$$

where ϕ is the phase shift of the pulse relative to P_o and Δp is the change in coherence level caused by the pulse ($\Delta p = p(t_i^+) - p(t_i^-)$).

Equation 11.48 shows that if a pulse produces a coherence jump of Δp, from σ^p to $\sigma^{p'}$, and if that pulse is phase shifted by an angle ϕ, then the coherence $\sigma^{p'}$ will be shifted in phase by $-i\Delta p\phi$ due to phase shifting of the pulse. This is the key step in phase encoding the magnetization for coherence selection.

11.3.1.2 Description of Coherence Pathways Using Coherence Jumps

Each coherence path in an experiment can be defined by either the coherences present during various time periods between pulses or *equivalently* by RF-pulse induced coherence jumps. The former description is useful for coherence selection with pulsed-field gradients while the latter is more useful for coherence selection by phase cycling of RF-pulses.

For example, in the COSY experiment there are three coherence paths that connect the initial state ($\rho = \sigma^0$) to the final detected coherence level, σ^{-1}. The location of these coherence jumps in the pulse sequence are shown in Fig. 11.8. The first two paths are desirable, while the third path will give rise to an artifact in the spectrum.

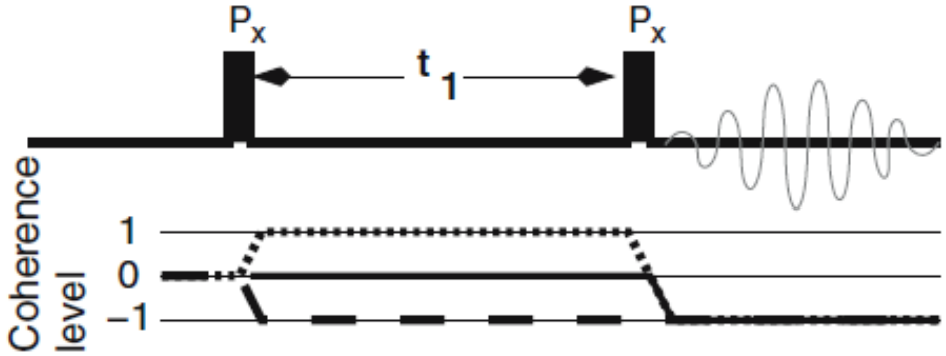

Figure 11.8. Coherence jumps in the COSY experiment. Three possible paths of coherence changes in the COSY experiment are illustrated. Note that only paths that end at a coherence level of -1 will give a detectable signal. The first path is represented by the dotted line and is described by coherence jumps of $\Delta p_1 = +1$, $\Delta p_2 = -2$. The second path is represented by the dashed line and consists of coherence jumps of $\Delta p_1 = -1$, $\Delta p_2 = 0$. Both of these paths will give rise to a normal COSY spectrum. The solid line shows the third undesired coherence path, with $\Delta p_1 = 0, \Delta p_2 = -1$.

Phase encoding of the different coherences can be achieved by changing the phase of the RF-pulses. The resultant phase shift of the coherence is the product of the phase shift of the RF-pulse, ϕ, and the change in coherence, Δp. Since a single coherence pathway is defined by a unique set of coherence jumps, it is possible to select out specific pathways by the appropriate phase cycling of pulses in much the same way gradients were used to select coherence paths. The phase shift that is associated with the desired pathway is refocused at the end of the experiment such that the desired coherence paths will add constructively to the overall signal.

The aggregate phase of the signal that is associated with a particular coherence path depends on the coherence jumps associated with that pathway and the phase shifts of the pulses at each coherence change. For every coherence path (j), the *change* in the coherence levels can be represented as a vector: $\vec{\Delta p}_j = (\Delta p_1, \Delta p_2, \ldots)$

For the first path listed above for the COSY experiment (Fig. 11.8): $\vec{\Delta p} = (+1, \ -2)$. The phase shifts associated with each RF-pulse can also be written as a vector:

$$\vec{\phi} = (\phi_1, \phi_2, \ldots)$$

The total phase shift that is accumulated over any particular coherence path, j, is just the dot product of these two vectors: $\Phi_j = \vec{\Delta P} \cdot \vec{\phi}$

For example, the total phase associated with the first coherence path in the COSY experiment is:

$$\Phi_1 = \Delta P_1 \phi_1 + \Delta P_2 \phi_2 = (+1) \times \phi_1 + (-2) \times \phi_2$$

In general, the signal associated with the j^{th} path is: $S_j = S_j^0 e^{-i\Phi_j}$
where S_j^o represents the signal that would be obtained with no phase shifting of pulses (e.g. $\vec{\phi} = 0$).

11.3.2 Selection of Coherence Pathways

The detected signal will contain a contribution for each coherence path in the experiment:

$$S = \sum_j S_j = \sum_j S_j^o e^{-i\Phi_j} \tag{11.54}$$

Using the COSY experiment discussed in Fig. 11.8 as an example, the final signal from any given scan is: $S = S_1^o e^{-i\Phi_1} + S_2^o e^{-i\Phi_2} + S_3^o e^{-i\Phi_3}$
The first two terms represent signals from desirable coherence paths, while the third term represents the signal from an undesirable path that will be eliminated by the phase cycle.

In contrast to coherence selection by pulsed-field gradients, the signals with different phases, S_j, do not cancel. Therefore, the selection of a particular coherence path is accomplished by the selection of pulse phases and receiver phase such that the desired signal always adds for each scan of the phase cycle while the signals from undesired paths sum to zero at the completion of the phase cycle.

11.3.2.1 Defining Phase cycles

The required phase shift associated with one pulse, ϕ, will depend on how many coherence jumps have to be filtered out by the particular pulse. A phase shift of:

$$\phi = \frac{k2\pi}{N} \quad k = 0,\ 1....(N-1)$$

will select out coherence orders: $\Delta p \pm nN$; $n = ..., -2, -1, 0, 1, 2, ...$, provided that the receiver phase is set to $-i\Delta p \times \phi$. This setting of the receiver phase will insure that desired signal will always appear as the real signal to the receiver, resulting in the co-addition of this signal over the entire phase cycle. In contrast, all other signals will sum to zero.

As an example, consider phase cycling of a single pulse with the intent of selecting a coherence change, Δp, of -2. If N is set to 3, corresponding to a three step phase cycle (pulse phases of 0, $2\pi/3$, and $4\pi/3$), and the receiver phase is set to 0, $-4\pi/3$, and $-8\pi/3$, then coherence jumps of -2 $\pm 3n$ will be retained, as shown in Fig. 11.9.

The result illustrated in Fig. 11.9 can be easily proven in general. First assume that an N-step phase cycle results in the positive selection of coherence jumps, $\Delta p \pm nN$. As an example let $\Delta p' = \Delta p + N$. To select this coherence jump it would be necessary to set the receiver phase to $e^{-i\Delta p\phi}$. This receiver phase is represented below by phase shifting the signal in the opposite direction, e.g. multiplying it by $e^{+i\Delta p\phi}$ (this term is underlined in Eq. 11.58). The detected signal will be the sum of all three signals, one for each phase of the pulse. The phase shift introduced in the signal by each RF-pulse is:

$$e^{-i\Delta p\frac{2\pi}{N}k}$$

where $k = 0, 1, 2$ and $N = 3$.

The net signal is given by the sum over the phase cycle:

$$\begin{aligned} S &= \sum_{k=0}^{N-1} e^{i\Delta p' \frac{2\pi}{N} k} S_0 e^{-i\Delta p \frac{2\pi}{N} k} = \sum_{k=0}^{N-1} e^{i(\Delta p + N)\frac{2\pi}{N} k} S_0 e^{-i\Delta p \frac{2\pi}{N} k} \\ &= \sum_{k=0}^{N-1} e^{i\Delta p \frac{2\pi}{N} k} e^{iN \frac{2\pi}{N} k} S_0 e^{-i\Delta p \frac{2\pi}{N} k} \qquad (11.58) \\ &= \sum_{k=0}^{N-1} e^{i\Delta p \frac{2\pi}{N} k} S_0 e^{-i\Delta p \frac{2\pi}{N} k} = N S_0 \end{aligned}$$

Now consider the case of rejection of the signal: $\Delta p' = \Delta p + m \quad m \neq N$

$$\begin{aligned} S &= \sum_{k=0}^{N-1} S_0 e^{i\Delta p' \frac{2\pi}{N} k} e^{-i\Delta p \frac{2\pi}{N} k} = S_0 \sum_{k=0}^{N-1} e^{i(\Delta p + m)\frac{2\pi}{N} k} e^{-i\Delta p \frac{2\pi}{N} k} \\ &= S_0 \sum_{k=0}^{N-1} e^{i\Delta p \frac{2\pi}{N} k} e^{im \frac{2\pi}{N} k} e^{-i\Delta p \frac{2\pi}{N} k} = S_0 \sum_{k=0}^{N-1} e^{im \frac{2\pi}{N} k} \\ &= 0 \end{aligned}$$

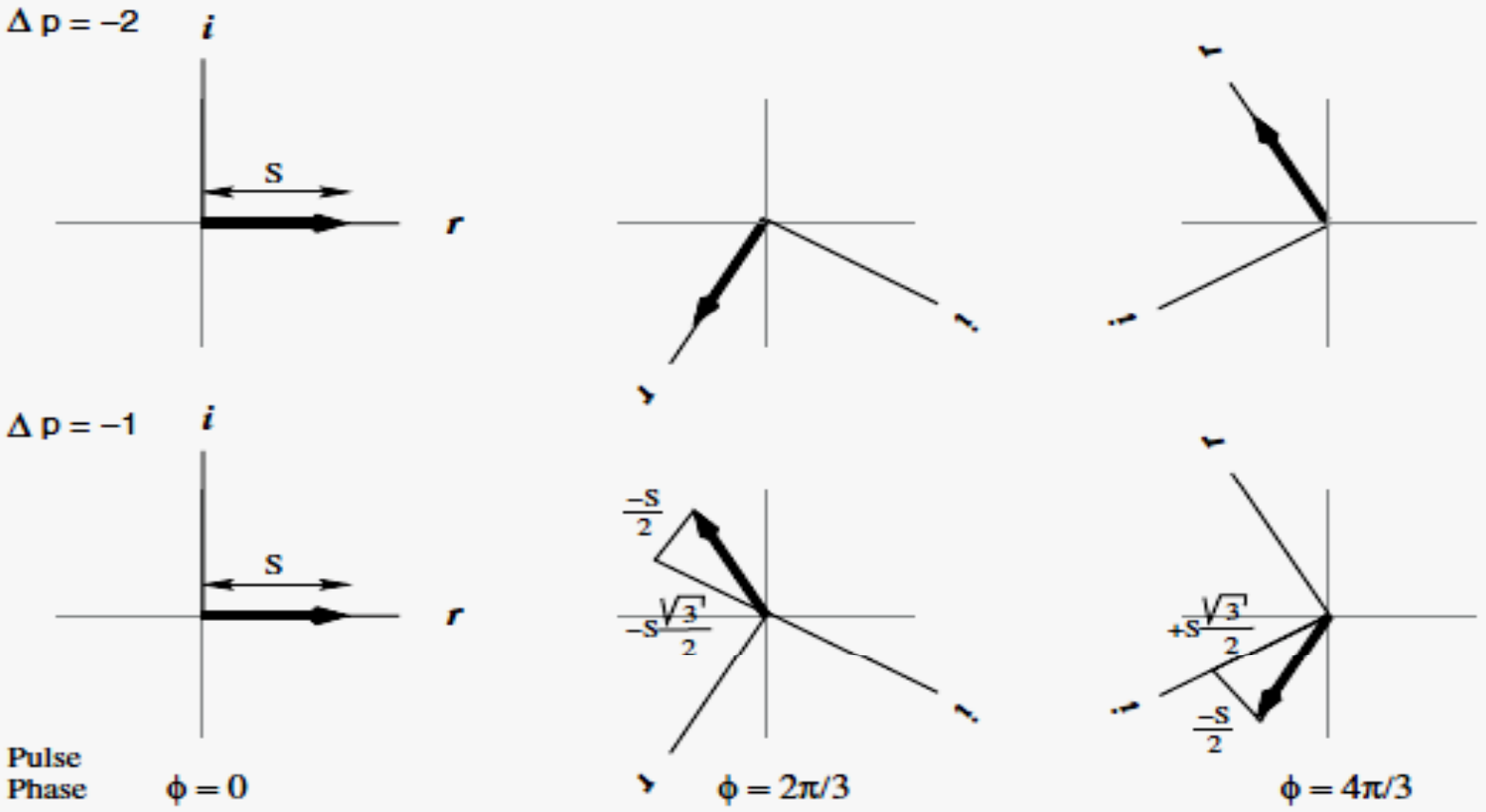

Pulse phase	*Signal*	*Phase of Receiver*	*Real Channel*	*Imaginary Channel*
$\Delta p = -2$				
0	$Se^{-i(-2)\cdot 0}$	0	S	0
$2\pi/3$	$Se^{-i(-2)\cdot 2\pi/3}$	$-(-2)\cdot 2\pi/3$	S	0
$4\pi/3$	$Se^{-i(-2)\cdot 4\pi/3}$	$-(-2)\cdot 4\pi/3$	S	0
Net sum			$3S$	0
$\Delta p = -1$				
0	$Se^{-i(-1)\cdot 0}$	0	S	0
$2\pi/3$	$Se^{-i(-1)\cdot 2\pi/3}$	$-(-2)\cdot 2\pi/3$	$-S/2$	$-S\frac{\sqrt{3}}{2}$
$4\pi/3$	$Se^{-i(-1)\cdot 4\pi/3}$	$-(-2)\cdot 4\pi/3$	$-S/2$	$+S\frac{\sqrt{3}}{2}$
Net sum			0	0

Figure 11.9. Selection and rejection of coherences in the COSY experiment by phase cycling. The upper series of diagrams show the signal for pulse phases of 0, $2\pi/3$, and $4\pi/3$ for a coherence jump of $\Delta p = -2$. The lower series of diagrams show the signal for a coherence jump of -1. The real and imaginary axis of the receiver are also indicated. The receiver phase is set to: $-\Delta p\phi$, where $-\Delta p$ is the desired coherence jump and ϕ is the phase of the RF-pulse. In this example, the receiver phase has been set to select the -2 coherence jump. Consequently, the signal associated with that coherence is always detected as the real signal by the receiver. In the case of a coherence jump of -1, the signal is not in phase with the receiver and the net sum of the real and imaginary channels is zero after completing all three scans of the phase cycle. The first column of the table shows the phase of the pulse, the second column shows the signal, including the phase shift introduced by the coherence jump and the change in the phase of the pulse. The third column shows the receiver phase setting for each scan. The last two columns show the signal for the real and imaginary channels, respectively. Note that the signals add in the case of $\Delta p = -2$ but cancel in the case of $\Delta p = -1$.

11.3.2.2 Example - Coherence Selection in the COSY Experiment

The coherence paths and associated coherence jumps in the COSY experiment are shown in Part A of Table 11.2. The first two give rise to the desired signal and the third needs to be suppressed by the phase cycling. It is necessary to retain both of the desirable paths to allow for quadrature detection during t_1 (see Chapter 12). Therefore, coherence jumps of ± 1 need to be retained from the first pulse, and jumps of -2, and 0 need to be retained from the second pulse. This selection will reject the coherence path $\sigma^o \rightarrow \sigma^0 \rightarrow \sigma^{-1}$ because that pathway is associated with coherence jumps of 0 and -1 for the first and second pulses, respectively.

The required Δp and number of steps (N) in the phase cycle are summarized in Table 11.2. In the case of the first pulse, $\Delta p = +1$ and it is necessary to set N=2 to select for both $\Delta p = +1$ and $\Delta p = -1$. For the second pulse $\Delta p = -2$ and N is set to 2 so that a coherence jump of 0 will also be selected. The receiver phase for each set of phase values is calculated from:

$$\varphi_{rec} = -i\vec{\Delta p}_j \cdot \vec{\phi} = -i(\Delta p_1 \phi_1 + \Delta p_2 \phi_2) \quad (11.63)$$

The pulse phases and associated receiver phases are given in part B of Table 11.2. Since the phase of each RF-pulse has to be cycled independently of the other, it is necessary to perform a four step phase cycle to obtain all possible permutations of the pulse phases (e.g. 2×2). The first two steps in the cycle serve to select the desired coherence jumps at the second pulse when the phase of the *first* pulse is 0. After the phase of the first pulse is changed to 2 (π), it is necessary to repeat the two-step

phase cycle of the second pulse to select the desired coherences at the second pulse. After all four steps of the phase cycle are summed the contribution of the undesired $\sigma^o \rightarrow \sigma^o \rightarrow \sigma^{-1}$ coherence path would be completely suppressed.

Table 11.2. Coherence changes and phase cycle in the COSY experiment. Part A of this table shows the three possible coherence paths, and the equivalent description of these pathways in terms of coherence jumps at each pulse in the experiment. The 1st and 2nd pathways should be retained by phase cycling and the last pathway needs to be suppressed. The lower part of the table indicates the Δp value and number of phase increments that are required to select the coherence jumps for *both* desired pathways. The coherence jumps that would be selected by these values of Δp and N are also shown.

A:

Coherence Path	*Coherence Jumps* (Δp)	
	1^{st} *Pulse*	2^{nd} *Pulse*
$\sigma^0 \rightarrow \sigma^{+1} \rightarrow \sigma^{-1}$	+1	- 2
$\sigma^0 \rightarrow \sigma^{-1} \rightarrow \sigma^{-1}$	-1	0
$\sigma^0 \rightarrow \sigma^{\ 0} \rightarrow \sigma^{-1}$	0	- 1
Δp	+1	- 2
Number of Steps (N)	2	2
Coherence jumps selected	$\Delta p = ... -3, -1, +1, +3...$	$\Delta p = ... -4, -2, 0, +2...$

Part B shows the four-step phase cycle of this experiment. The phases for the RF-pulses, and the associated receiver phases, are shown. The short-hand notation for pulse and receiver phases is: $0 = 0$, $\pi/2 = 1$, $\pi = 2$, $3\pi/2 = 3$. The receiver phase is calculated using Eq. 11.63, using $\Delta p_1 = +1$ and $\Delta p_2 = -2$. For example, the third step of the phase cycle has pulse phases of $\phi_1 = \pi$ and $\phi_2 = 0$, therefore the receiver phase is: $\varphi_{rec} = -[(+1)(\pi) + (-2)(0)] = -\pi = \pi$. This phase is represented by a 2 in the table.

B:

	Phase Cycle Step			
	1	2	3	4
First Pulse	0	0	2	2
Second Pulse	0	2	0	2
Receiver Phase (φ_{rec})	0	0	2	2

11.3.3 Phase Cycling in the HMQC Pulse Sequence

Phase cycling can also be used for coherence editing in heteronuclear pulse sequences. To simplify the analysis, the coherence order changes are followed independently for each type of spin. In contrast to coherence selection with gradients, the phase shifts in the coherences that are introduced by phase cycling are *independent* of the type of nucleus. Consequently, the overall receiver phase that is required to select the desired coherence pathways is simply $-i\vec{\Delta p} \cdot \vec{\phi}$.

Coherence levels in the HMQC Experiment

The HMQC pulse sequence is shown in Fig. 11.10. The coherence levels that are present at various locations in the sequence can be inferred from the Cartesian representation of the density matrix:

$$\begin{array}{ccccccccccccc} I_z & \overset{P_{90}^H}{\rightarrow} & -I_y & \overset{\Delta}{\rightarrow} & I_xS_z & \overset{P_{90}^S}{\rightarrow} & \frac{t_1}{2}\ 180^\circ_H\ \frac{t_1}{2} & \overset{}{\rightarrow} & P_{90}^S & \overset{}{\rightarrow} & I_xS_z & \overset{\Delta}{\rightarrow} & I_y \\ \sigma^o & & \sigma_H^{\pm 1} & & & & \sigma_H^{\pm 1} + \sigma_S^{\pm 1} & & & & \sigma_H^{\pm 1} & & \end{array}$$

The coherence changes in the HMQC experiment are illustrate in Fig. 11.10. The first proton pulse creates single quantum proton coherence. The next heteronuclear pulse generates single-quantum X-nucleus coherence that persists throughout the t_1 labeling period. During the t_1 period the 180° pulse on the proton converts the σ_H^{+1}

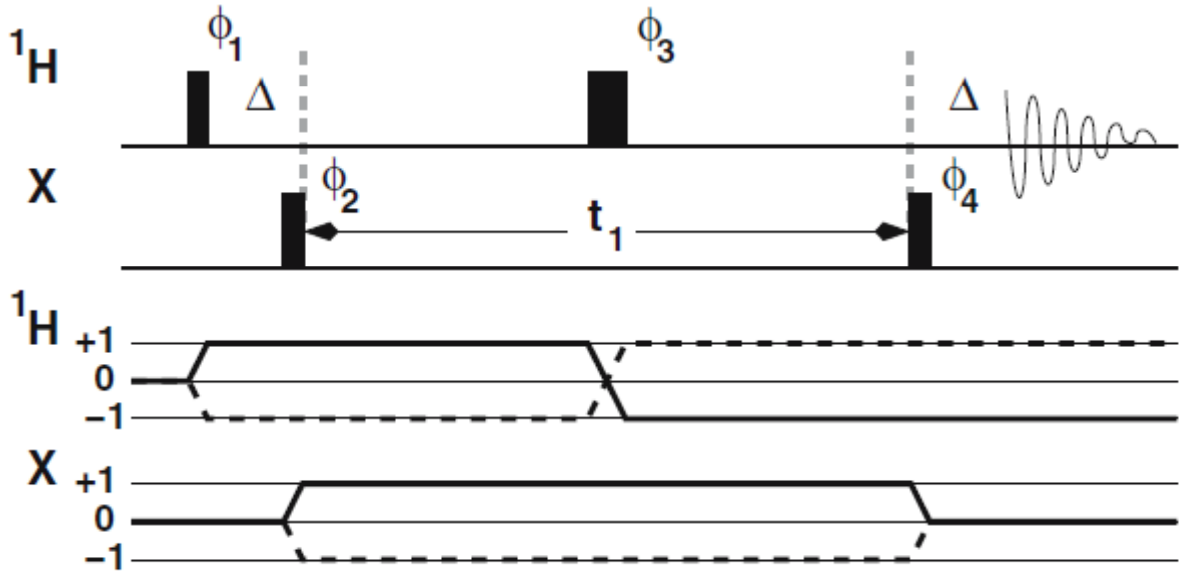

Figure 11.10 Coherence jumps in the HMQC experiment. The separate coherence jumps for the proton and heteronuclear spin are shown for an HMQC experiment. The solid line and the dashed line show the coherence paths that are to be retained by phase cycling.

coherence to σ_H^{-1} coherence, a net change of ± 2. This two level change in the coherence can be understood by writing I_x as the sum of the raising and lowering operators:

$$I_x = \frac{1}{2}(I^+ + I^-)$$

The effect of the 180° pulse on I^+ is: $I^+ = I_x + iI_y \rightarrow I_x - iI_y = I^-$

or a net change in coherence of -2.

The single quantum coherence associated with the X-nucleus is returned to zero quantum coherence by the second heteronuclear pulse, and the density matrix refocuses to single quantum coherence by the end of the Δ delay.

Defining the Phase Cycle

The first proton pulse is generally not phase cycled since imperfections in this pulse cannot give rise to detectable magnetization. The phases of the three remaining pulses are cycled to remove artifacts. The desired coherence jumps and number of phase shifts that are associated with each pulse are shown in Table 11.3.

The coherence jump associated with the first X-nucleus pulse is +1. However, since a jump of -1 must also be preserved, a two step phase cycle is required. In a similar manner, the desired coherence jumps associated with the last X-nucleus pulse is either -1 (solid line in Fig. 11.10) or +1 (dotted line), required a two step phase cycle. A total of four steps ($N = 4$) are required for the proton 180° pulse since the desired coherence changes are either -2 or +2. Choosing a Δp of +2, and $N = 4$, insures that

only Δp values of -2 and +2 will be retained. Note that coherence jumps of -6 and +6 are also retained by this selection since $\Delta p = \Delta p \pm N$, but such high coherence levels cannot be attained with two coupled spins.

Since each phase cycle operates independently of the other phase cycles, a total of 16 scans are required ($2 \times 4 \times 2$) to suppress all of the artifacts. The complete phase cycle, including the receiver phase, is shown in Table 11.3.

		Experiment Number															
Pulse	Δp	1	2	3	4	5	6	7	8	9	10	11	12	13	14	15	16
2	1	0	2	0	2	0	2	0	2	0	2	0	2	0	2	0	2
3	2	0	0	1	1	2	2	3	3	0	0	1	1	2	2	3	3
4	1	0	0	0	0	0	0	0	0	2	2	2	2	2	2	2	2
φ_{rec}	-	0	2	2	0	0	2	2	0	2	0	0	2	2	0	0	2

Table 11.3. Phase cycle of the HMQC experiment. The desired coherence jumps are shown in the second column from the left. Note that the first proton pulse (ϕ_1) is not phase cycled. The first heteronuclear pulse (ϕ_2) should generate a ± 1 coherence jump from the initial σ_X^0. The allowed coherence jumps that are associated with the proton 180° pulse are ± 2 and those associated with the final heteronuclear pulse are -1 for σ_X^{+1} and +1 for σ_X^{-1}. The receiver phase, φ_{rec}, is calculated from $-\vec{\Delta p} \cdot \vec{\phi}$. For example, the phase of the receiver for the 16^{th} pulse is: $-[(1)(2) + (2)(3) + (1)(2)] = -10 = -2 = +2$.